Anomalous Hall Effect in Magnetite: Universal Scaling Relation Between Hall and Longitudinal Conductivity in Low-Conductivity Ferromagnets

Deepak Venkateshvaran,[1, 2] Wolfgang Kaiser,[1] Andrea Boger,[1] Matthias Althammer,[1] M.S. Ramachandra Rao,[2] Sebastian T. B. Goennenwein,[1] Matthias Opel,[1, *] and Rudolf Gross[1, 3, †]

[1]*Walther-Meißner-Institut, Bayerische Akademie der Wissenschaften, 85748 Garching, Germany*
[2]*Materials Science Research Centre, Indian Institute of Technology Madras, Chennai 600036, India*
[3]*Physik-Department, Technische Universität München, 85748 Garching, Germany*
(Dated: May 8, 2008)

The anomalous Hall effect (AHE) has been studied systematically in the low-conductivity ferromagnetic oxide $Fe_{3-x}Zn_xO_4$ with $x = 0$, 0.1, and 0.5. We used (001), (110), and (111) oriented epitaxial $Fe_{3-x}Zn_xO_4$ films grown on MgO and sapphire substrates in different oxygen partial pressure to analyze the dependence of the AHE on crystallographic orientation, Zn content, strain state, and oxygen deficiency. Despite substantial differences in the magnetic properties and magnitudes of the anomalous Hall conductivity $\sigma_{xy}^{\mathrm{AHE}}$ and the longitudinal conductivity σ_{xx} over several orders of magnitude, a universal scaling relation $\sigma_{xy}^{\mathrm{AHE}} \propto \sigma_{xx}^{\alpha}$ with $\alpha = 1.69 \pm 0.08$ was found for all investigated samples. Our results are in agreement with recent theoretical and experimental findings for ferromagnetic metals in the dirty limit, where transport is by metallic conduction. We find the same scaling relation for magnetite, where hopping transport prevails. The fact that this relation is independent of crystallographic orientation, Zn content, strain state, and oxygen deficiency suggests that it is universal and particularly does not depend on the nature of the transport mechanism.

PACS numbers: 75.47.-m, 72.25.-b, 73.50.-h, 75.47.Pq

The physics of the Hall effect in ferromagnetic materials is discussed intensively and controversially since the 1950s. Early experimental work on ferromagnetic metals suggested that the Hall resistivity can be described by the empirical relation $\rho_{xy} = R_O\mu_0 H + R_A\mu_0 M$, where H is the applied magnetic field and M the spontaneous magnetization of the ferromagnet. The first term, proportional to H and characterized by the ordinary Hall coefficient R_O, describes the ordinary Hall effect (OHE), whereas the second term, proportional to M and characterized by the anomalous Hall coefficient R_A, represents the anomalous Hall effect (AHE). Although the AHE is generally observed in ferromagnetic metals and semiconductors, its origin has been one of the most intriguing and controversial issues in solid-state physics and various theories based on intrinsic and extrinsic mechanisms have been proposed [1, 2, 3, 4, 5]. Whereas the extrinsic origins of the AHE are based on skew scattering [2, 3] and side jump [4, 5] mechanisms due to spin orbit interaction connecting the spin polarization with the orbital motion of electrons, the intrinsic origin of the AHE is closely related to the Berry phase [6] of the Bloch electrons [1, 7, 8, 9, 10, 11, 12, 13]. The dissipationless and topological nature of the intrinsic mechanism has attracted much attention recently and various first principles band structure calculations have been performed to explain the AHE in transition metals [14, 15], ferromagnetic semiconductors [9, 10, 16], and oxides [17, 18, 19, 20].

A powerful experimental test for AHE models is the measurement of the scaling of the anomalous Hall resistivity (conductivity) ρ_{xy}^{AHE} ($\sigma_{xy}^{\mathrm{AHE}}$) with the longitudinal resistivity (conductivity) ρ_{xx} (σ_{xx}). The skew scattering

and side jump mechanisms are known to yield $\rho_{xy}^{\mathrm{AHE}} \propto \rho_{xx}$ ($\sigma_{xy}^{\mathrm{AHE}} \propto \sigma_{xx}$) and $\rho_{xy}^{\mathrm{AHE}} \propto \rho_{xx}^2$ ($\sigma_{xy}^{\mathrm{AHE}} \sim const.$), respectively. Recently, a unified theory of the AHE has been developed for multiband ferromagnetic metals with dilute impurities, taking into account resonant contributions from band crossings. This model predicts three scaling regimes as a function of electron scattering time. In the clean limit the skew scattering mechanism dominates resulting in $\sigma_{xy}^{\mathrm{AHE}} \propto \sigma_{xx}$. On decreasing scattering time or conductivity, the intrinsic contribution becomes dominant, yielding $\sigma_{xy}^{\mathrm{AHE}} \simeq const$. In the dirty limit, the intrinsic contribution is strongly damped, resulting in a scaling relation $\sigma_{xy}^{\mathrm{AHE}} \propto \sigma_{xx}^{1.6}$ [12, 13]. The crossover between the intrinsic and dirty limit regime has been observed very recently for several itinerant ferromagnets [21]. Furthermore, the $\sigma_{xy}^{\mathrm{AHE}} \propto \sigma_{xx}^{1.6}$ scaling has been found for several low-conductivity materials independent of the details of the underlying transport mechanism (hopping or metallic conduction) [21, 22, 23, 24, 25]. This is quite surprising and not understood in detail so far. Although theoretical models have been proposed for the AHE in low-conductivity ferromagnetic materials [10, 17], where transport is dominated by hopping, or in the Hall insulator phase [26], no complete theoretical understanding has been developed. In particular, no universal scaling behavior independent of the underlying transport mechanism has been predicted.

In this Letter, we address the question whether or not the scaling relation $\sigma_{xy}^{\mathrm{AHE}} \propto \sigma_{xx}^{1.6}$ predicted for ferromagnetic metals in the dirty limit [12, 13] and quantum Hall insulators [26] also holds for low-conductivity ferromagnetic oxides with hopping type conductivity as indicated

by recent experiments [24, 25]. To do so we performed a systematic study of the AHE in magnetite (Fe_3O_4), which belongs to this material class. In particular, we checked whether the scaling relation is universal or depends on the specific sample properties. In order to clarify possible influences of the crystal structure, the charge carrier density, or Zn content we studied (i) epitaxial Fe_3O_4 films with (001), (110), and (111) orientation, (ii) films grown under different oxygen partial pressure resulting in different amounts of oxygen vacancies, and (iii) $Fe_{3-x}Zn_xO_4$ films with $x = 0.1$ and 0.5. Although the magnetic properties such as saturation magnetization and coercivity differ significantly among the various samples and the absolute conductivity values range over four orders of magnitude, the same scaling relation $\sigma_{xy}^{\mathrm{AHE}} \propto \sigma_{xx}^{\alpha}$ with $\alpha = 1.69 \pm 0.08$ is observed for all samples providing evidence that this scaling relation is indeed universal.

Epitaxial thin films of $Fe_{3-x}Zn_xO_4$ with $x = 0$, 0.1, and 0.5 were grown by laser molecular beam epitaxy [27, 28] at a base pressure of 3.7×10^{-3} mbar in pure Ar atmosphere or an Ar/O_2 (99:1) mixture. We used MgO(001), MgO(110), and Al_2O_3(0001) substrates to obtain (001), (110), and (111) oriented films with different amount of epitaxial coherency strain, respectively. Details of the growth process are given elsewhere[29, 30, 31]. X-ray diffraction reveals a high epitaxial quality of our samples as demonstrated by a FWHM of the rocking curves of the (004) reflection smaller than $0.05°$. X-ray reflectometry was used to get precise values of the film thickness ranging between 30 and 60 nm. Magnetic characterization was performed by SQUID magnetometry. For magnetotransport measurements the films were patterned into typically $45\,\mu m$ wide and $350\,\mu m$ long Hall bars by optical lithography and Ar ion beam milling [32]. The Hall bars were aligned parallel to the in-plane $\langle 100 \rangle$ directions
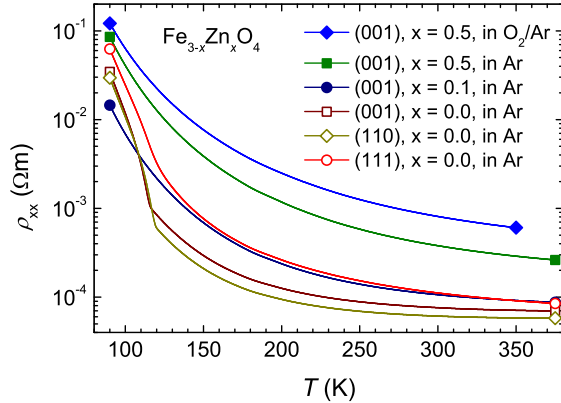

FIG. 1: (color online) Longitudinal resistivity versus temperature for epitaxial $Fe_{3-x}Zn_xO_4$ films. The (001), (110), and (111) oriented films were grown on MgO(001), MgO(110), and Al_2O_3(0001) substrates.

for the (001) and (110) films and also along the $\langle 110 \rangle$ directions for the (110) films, and parallel to the [1-10] and [11-2] directions for the (111) films.

Magnetotransport measurements as a function of temperature T and magnetic field H were performed using a standard 4-probe technique with H applied perpendicular to the film plane. The Hall resistivity ρ_{xy} was obtained by anti-symmetrization of the values measured for opposite magnetic field directions to eliminate offsets due to contact potential or a geometric misalignment of the Hall probes. The respective conductivities were derived by inversion of the resistivity tensor. For cubic symmetry and $H \| z$, we get

$$\sigma_{xx} = \frac{\rho_{xx}}{\rho_{xx}^2 + \rho_{xy}^2} \simeq 1/\rho_{xx} \qquad (1)$$

$$\sigma_{xy} = \frac{\rho_{xy}}{\rho_{xx}^2 + \rho_{xy}^2} \simeq \frac{\rho_{xy}}{\rho_{xx}^2} \;, \qquad (2)$$

since $\rho_{xy} \ll \rho_{xx}$ for our samples.

We first discuss $\rho_{xx}(T)$ for the different films. As shown in Fig. 1, ρ_{xx} increases by more than two orders of magnitude on decreasing T from 350 to below 100 K. Furthermore, ρ_{xx} sensitively depends on the Zn-doping, the growth atmosphere and the crystallographic orientation. An increasing Zn content increases resistivity. This is caused by the substitution of Fe^{3+} by Zn^{2+} ions reducing the carrier concentration [33, 34]. Zn-substitution also smears out the Verwey transition [35] which is clearly seen for the undoped samples as a pronounced increase of resistivity at $T_V \simeq (115 \pm 5)$ K. This temperature is slightly smaller than the ideal bulk value (120 K) and also the increase in ρ_{xx} is less sharp than for bulk samples what can be attributed to the nonvanishing epitaxial strain [36]. It is also seen that the resistivity increases by growing the films in an Ar/O_2 mixture. This is due to a reduction of oxygen vacancies resulting in a decrease of the carrier density.

The Hall resistivity ρ_{xy} is plotted versus H in Fig. 2 at $T = 300$ K together with the magnetization curves of the same films. Similar curves are obtained at other temperatures. It is evident that ρ_{xy} scales with magnetization M. This is expected according to the empirical relation $\rho_{xy} = \rho_{xy}^{\mathrm{OHE}} + \rho_{xy}^{\mathrm{AHE}} = R_O \mu_0 H + R_A \mu_0 M$, if the anomalous contribution ρ_{xy}^{AHE} dominates. In Fig. 3 we have plotted $\rho_{xy}(H)$ at 200 K up to 14 T. The data show the already discussed behavior following the $M(H)$ curves due to the dominating anomalous Hall contribution. We also note that the initial slope of the $\rho_{xy}(H)$ curves can be larger than $1\,\mu\Omega m/T$ corresponding to a sensitivity of more than $100\,V/AT$ for a 10 nm thick film in agreement with a recent report [25]. To derive $\rho_{xy}^{\mathrm{AHE}}(M_s) = R_A \mu_0 M_s$, where M_s is the saturation magnetization, from the measured $\rho_{xy}(H)$ curve, one has to separate the ordinary and anomalous contributions. If M saturates at high fields, this can be simply done by extrapolation of the linear high field part of $\rho_{xy}(H)$ back
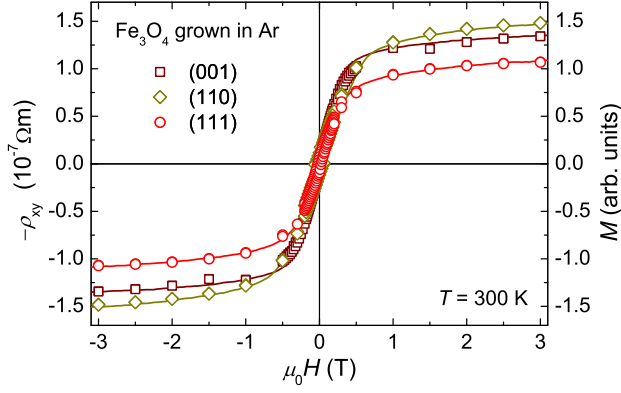
FIG. 2: (color online) Room temperature Hall resistivity (lines) and magnetization (symbols) plotted versus the magnetic field applied perpendicular to the film plane for epitaxial (001), (110), and (111) oriented Fe_3O_4 films grown on MgO(001), MgO(110), and Al_2O_3(0001) substrates.

to $H = 0$, yielding $\rho_{xy}^{\mathrm{AHE}}(H = 0) = \rho_{xy}^{\mathrm{AHE}}(M = M_s)$. Unfortunately, such straightforward analysis is not possible for magnetite, since M does not fully saturate up to fields of the order of $10\,\mathrm{T}$ due to anti-phase boundaries [37]. Fortunately, $\rho_{xy}^{\mathrm{OHE}} \sim 2 \times 10^{-9}\,\Omega\mathrm{m}$ at $1\,\mathrm{T}$ [25, 31] is very small and therefore can be safely neglected compared to the about two orders of magnitude larger contribution ρ_{xy}^{AHE} of the AHE. Then, in good approximation we can use $\rho_{xy}^{\mathrm{AHE}}(H = 0) = \rho_{xy}^{\mathrm{AHE}}(M_s) \simeq \rho_{xy}(14\,\mathrm{T})$. The corresponding anomalous Hall conductivity is derived as $\sigma_{xy}^{\mathrm{AHE}} = \rho_{xy}^{\mathrm{AHE}}(0)/\rho_{xx}^2(0)$.

By varying the crystallographic orientation, the growth atmosphere, and the Zn content we have fabricated epitaxial $Fe_{3-x}Zn_xO_4$ films with $\sigma_{xy}^{\mathrm{AHE}}$ and σ_{xx} values ranging over almost five and three orders of magnitude, respectively, in the studied temperature regime from 90

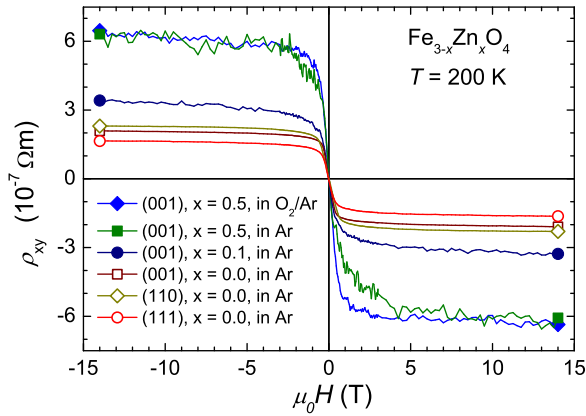FIG. 3: (color online) Hall resistivity ρ_{xy} plotted versus magnetic field applied perpendicular to the film plane at $200\,\mathrm{K}$ for six different $Fe_{3-x}Zn_xO_4$ films.
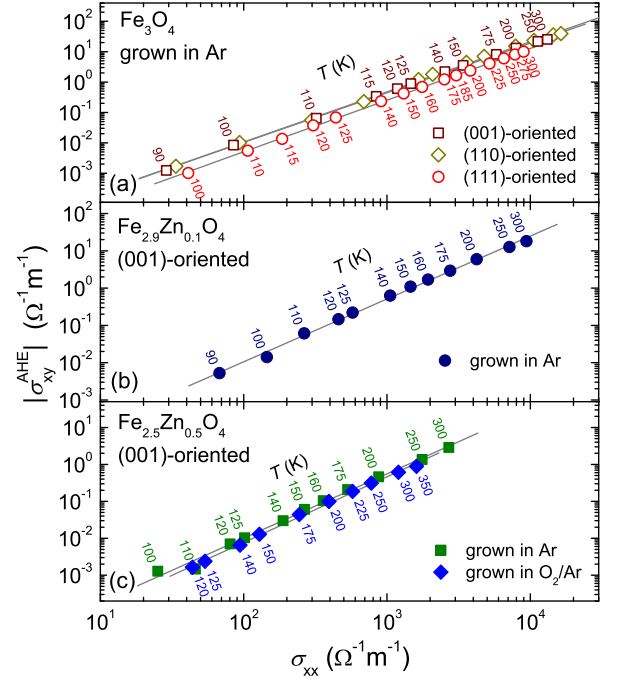

FIG. 4: (color online) Modulus of the anomalous Hall conductivity, $|\sigma_{xy}^{\mathrm{AHE}}|$, plotted versus longitudinal conductivity σ_{xx} in a double logarithmic representation for different epitaxial $Fe_{3-x}Zn_xO_4$ films in the temperature regime between 90 and $350\,\mathrm{K}$. The lines are linear fits to the data.

to $350\,\mathrm{K}$. The most intriguing result is that irrespective of these pronounced differences all data follow the same scaling plot (see Fig. 4)

$$\left|\sigma_{xy}^{\mathrm{AHE}}\right| = a \cdot \sigma_{xx}^{\alpha} \qquad (3)$$

with $\alpha = 1.69 \pm 0.08$ and $a = (4 \pm 2) \times 10^{-6}[1/\Omega\mathrm{m}]^{1-\alpha}$. This scaling behavior even holds on moving across the Verwey transition, which is associated with a structural phase transition (cubic to monoclinic) as well as charge and/or orbital ordering [38, 39]. With respect to the scaling exponent α our systematic data is in good agreement with theoretical predictions [12, 13]. Some data even indicate a tendency towards saturation of $\sigma_{xy}^{\mathrm{AHE}}$ at conductivity values above $10^4\Omega^{-1}\mathrm{m}^{-1}$. Our results also agree well with those obtained on polycrystalline [40] and epitaxial Fe_3O_4 films of different thickness [25] as well as those obtained from single crystals [41]. We further note that scaling relations with about the same exponent but different prefactors have been found for $Ti_{1-x}Co_xO_{2-\delta}$ [22] and a number of other oxide materials [17, 21, 23, 24]. This strongly suggests that the observed scaling behavior in low-conductivity ferromagnetic oxides is universal and not related to details of the crystal structure and crystallographic orientation, doping level, oxygen stoichiometry, strain state, or density of anti-phase boundaries.

The origin of the observed universal scaling relation is still controversial. Although a recent theoretical model

[12, 13] developed for multiband ferromagnetic metals with dilute impurities predicts $\sigma_{xy}^{\mathrm{AHE}} \propto \sigma_{xx}^{1.6}$ in the dirty limit, this model does not cover the case of low-conductivity ferromagnetic oxides where electric transport is dominated by hopping. Furthermore, it is still unclear to what extent the model developed for quantum Hall insulators [26] can be applied. In any case, our results together with the available literature data [21, 22, 24, 25] suggest that the scaling relation holds for low-conductivity materials independent of the details of the specific material parameters and the underlying transport mechanism (hopping or metallic conduction) and therefore can be considered universal.

In summary, we have performed a systematic study of the AHE in the low-conductivity ferromagnetic oxide $\mathrm{Fe}_{3-x}\mathrm{Zn}_x\mathrm{O}_4$. Independent of the crystallographic orientation, Zn content, oxygen deficiency, and strain state, resulting in substantial differences in magnetic and magnetotransport properties, a universal scaling relation $\sigma_{xy}^{\mathrm{AHE}} \propto \sigma_{xx}^{\alpha}$ with $\alpha = 1.69 \pm 0.08$ was found. Comparing our results with recent literature data we can conclude that the observed scaling relation is very general and holds for low-conductivity ferromagnetic materials irrespective of the details of the underlying transport mechanism.

------

* Electronic address: Matthias.Opel@wmi.badw.de

† Electronic address: Rudolf.Gross@wmi.badw.de

[1] R. Karplus and J. M. Luttinger, Phys. Rev. **95**, 1154 (1954).

[2] J. Smit, Physica (Amsterdam) **21**, 877 (1955); **24**, 39 (1958).

[3] J.M. Luttinger, Phys. Rev. **112**, 739 (1958).

[4] L. Berger, Phys. Rev. B **2**, 4559 (1970); Phys. Rev. B **5**, 4559 (1970).

[5] P. Nozières and C. Lewiner, J. Phys. (Paris) **34**, 901 (1973).

[6] M. V. Berry, Proc. R. Soc. London, Ser. A **392**, 45 (1984).

[7] G. Sundaram, Q. Niu, Phys. Rev. B **59**, 14915 (1999).

[8] S. Onoda, N. Nagaosa, J. Phys. Soc. Jpn. **71**, 19 (2002).

[9] T. Jungwirth, Q. Niu, A.H. MacDonald, Phys. Rev. Lett. **88**, 207208 (2002).

[10] A.A. Burkov, L. Balents, Phys. Rev. Lett. **91**, 057202 (2003).

[11] N. Nagaosa, J. Phys. Soc. Jpn. **75**, 042001 (2006).

[12] S. Onoda, N. Sugimoto, N. Nagaosa, Phys. Rev. Lett. **97**, 126602 (2006).

[13] S. Onoda, N. Sugimoto, N. Nagaosa, Phys. Rev. B **77**, 165103 (2008).

[14] Y. Yao, L. Kleinman, A.H. MacDonald, J. Sinova, T. Jungwirth, Ding-sheng Wang, E. Wang, Q. Niu, Phys. Rev. Lett. **92**, 037204 (2004)

[15] S.A. Baily, M.B. Salamon, Phys. Rev. B **71**, 104407 (2005).

[16] C. Zeng, Y. Yao, Q. Niu, H.H. Weitering, Phys. Rev. Lett. **96**, 037204 (2006).

[17] Y. Lyanda-Geller, S. H. Chun, M. B. Salamon, P. M. Goldbart, P. D. Han, Y. Tomioka, A. Asamitsu, Y. Tokura, Phys. Rev. B **63**, 184426 (2001).

[18] Z. Fang, N. Nagaosa, K.S. Takahashi, A. Asamitsu, R. Mathieu, T. Ogasawara, H. Yamada, M. Kawasaki, Y. Tokura, K. Terakura, Science **302**, 92 (2003).

[19] R. Mathieu, A. Asamitsu, H. Yamada, K. S. Takahashi, M. Kawasaki, Z. Fang, N. Nagaosa, Y. Tokura Phys. Rev. Lett. **93**, 016602 (2004).

[20] L. M. Wang Phys. Rev. Lett. **96**, 077203 (2006).

[21] T. Miyasato, N. Abe, T. Fujii, A. Asamitsu, S. Onoda, Y. Onose, N. Nagaosa, Y. Tokura, Phys. Rev. Lett. **99**, 086602 (2007).

[22] H. Toyosaki, T. Fukumura, Y. Yamada, K. Nakajima, T. Chikyow, T. Hasegawa, H. Koinuma, and M. Kawasaki, Nature Mater. **3**, 221 (2004).

[23] K. Ueno, T. Fukumura, H. Toyosaki, M. Nakano, and M. Kawasaki, Appl. Phys. Lett. **90**, 072103 (2007).

[24] T. Fukumura, H. Toyosaki, K. Ueno, M. Nakano, T. Yamasaki, and M. Kawasaki, J. J. Appl. Phys. **46**, L642 (2007).

[25] A. Fernández-Pacheco, J. M. De Teresa, J. Orna, L. Morellon, P. A. Algarabel, J. A. Pardo, and M. R. Ibarra, Phys. Rev. B **77**, 100403(R) (2008).

[26] L.P. Pryadko, A. Auerbach, Phys. Rev. Lett. **82**, 1253 (1999).

[27] R. Gross *et al.*, in *Superconducting and Related Oxides: Physics and Nanoengineering IV*, edited by D. Pavuna and I. Bosovic (SPIE Conf. Proc. 4058, 278, 2000).

[28] J. Klein, C. Höfener, L. Alff, and R. Gross, Supercond. Sci. **12**, 1023–1027 (1999).

[29] D. Reisinger, B. Blass, J. Klein, J. B. Philipp, M. Schonecke, A. Erb, L. Alff, and R. Gross, Appl. Phys. A **77**, 619 (2003).

[30] D. Reisinger, M. Schonecke, T. Brenninger, M. Opel, A. Erb, L. Alff, R. Gross, J. Appl. Phys. **94** 1857 (2003).

[31] D. Reisinger, P. Majewski, M. Opel, L. Alff, R. Gross, Appl. Phys. Lett. **85**, 4980 (2004).

[32] L. Alff *et al.*, Physica C **200**, 277 (1992).

[33] J. Takaobushi *et al.*, Appl. Phys. Lett. **89**, 242507 (2006).

[34] J. Takaobushi *et al.*, Phys. Rev. B **76**, 205108 (2007).

[35] E. J. W. Verwey, Nature (London) **144**, 327 (1939).

[36] X. Li, A. Gupta, G. Xiao, G. Gong, J. Appl. Phys. **83**, 7049 (1998).

[37] D. T. Margulies *et al.*, Phys. Rev. Lett. **79**, 5162 (1997); D. T. Margulies *et al.*, Phys. Rev. B **53**, 9175 (1996).

[38] J. García, G. Subías, M. G. Proietti, J. Blasco, H. Renevier, J. L. Hodeau, and Y. Joly, Phys. Rev. B **63**, 054110 (2001).

[39] F. Walz, J. Phys.: Condens. Matter **14**, R285-R340 (2002).

[40] J. S. Feng, R. D. Pashley, and M. A. Nicolet, J. Phys. C: Solid State Phys. **8**, 1010 (1975).

[41] S. Todo, K. Siratori, and S. Kimura, J. Phys. Soc. Japan **64**, 2118 (1995).